

Gravitational Lensing of High Redshift Type Ia Supernova: A Probe of Medium Scale Structure

R. Benton Metcalf

*Departments of Physics and Astronomy, and Center for Particle Astrophysics
University of California, Berkeley, California 94720*

ABSTRACT

Gravitational lensing will magnify and demagnify high redshift type Ia supernovae. The dispersion in the peak magnitudes due to this effect approaches the size of the intrinsic dispersion at $z \gtrsim 1$. I propose a statistical method for measuring this effect. It is shown that the added dispersion is related to $a^{-2}kP(k)$ which makes it sensitive to halo scale density structure - smaller scale structure than is accessible to measurements of lensing by large scale structure through galaxy shear. Using cold dark matter models it is estimated that the amount and quality of data needed is attainable in the next few years. A parameterization of the signal is motivated by these models. The signal is found to be highly dependent on scales where structure is nonlinear and weakly dependent on the Hubble parameter. The lensing's redshift dependence is related to the evolution of medium scale structure between the present and $z \sim 0.5 - 1.5$. The skewness of the magnification distribution is discussed and interpreted in terms of the density of nonlinear structures. The statistical method proposed could also be used to look for other sources of redshift evolution in the properties of type Ia supernovae.

1. Introduction

There is presently a large effort underway to predict and detect the weak gravitational lensing caused by Large Scale Structure (LSS) or the “cosmic shear” (see (Valdes, Tyson & Jarvis 1983), (Mould *et al.* 1994), (Villumsen 1996), (Kaiser 1992), (Kaiser 1996)). Such a measurement would constitute a direct probe of the mass density fluctuations on large scales irrespective of how light and baryons are distributed. This would make it possible to measure one of cosmology’s least well understood processes, how light traces mass and whether this is a function of scale. Gravitational lensing causes images to be both magnified and demagnified as well as stretched asymmetrically (shear). Most of the methods proposed for detecting LSS lensing are based on measuring the shear in high redshift galaxy images. Although the distortions in the ellipticities of individual galaxies are expected to be small they are distorted in coherent ways. Indications of lensing are sought in the alignment of the galaxy images with the assumption that they are not intrinsically aligned. This technique has already been used with great success on galaxy cluster lensing. We propose in this paper a method of detecting lensing by LSS, but at a somewhat smaller scale than galaxy lensing.

The study of high redshift supernovae is another area of cosmology and astrophysics that has seen a lot of activity lately. Type Ia supernovae, the brightest type of supernova, are believed to be caused by the thermonuclear explosion of an accreting white dwarf. It has been found empirically that the peak magnitude of type Ia’s have a dispersion of only 0.2 - 0.3 mag in B band. It has further been found that the peak magnitude is related to the width of the supernova’s light-curve which can then be used to reduce the dispersion to about 0.17 mag if one color is used (Hammuy *et al.* 1996) and 0.12 mag if multiple colors are used (Riess, Press & Kirshner 1996). In addition to the light-curve width, the supernova’s color and spectral features are related to the peak luminosity (Branch, Nugent & Fisher 1997, Nugent *et al.* 1995). It may be possible to reduce the dispersion to below 0.1 mag in the future. This uniformity in type Ia supernovae combined with their high luminosity makes them an excellent tool for doing cosmology. Using them to measure the redshift-luminosity distance relation has recently resulted in tightened constraints on

the cosmological parameters Ω and Ω_Λ (Perlmutter *et al.* 1997), (Perlmutter *et al.* 1998), (Garnavich *et al.* 1998). There are now systematic searches for Ia supernovae at high redshift which can reliably discover on the order of ten supernovae in two nights of observing and do spectroscopic followup (Perlmutter *et al.* 1997). In addition there are several ongoing searches for low redshift supernovae. To date there have been more than 100 type Ia supernovae discovered with redshifts between $z = 0.4$ and 0.97 and many additional ones at lower redshift.

Supernovae will be magnified or demagnified by any nonhomogeneous mass distribution that happens to lie near our line of sight. Being point sources the shear in supernovae images will not be observable. If the mass responsible for the lensing is in compact objects ($\gtrsim 10^{-3} M_\odot$) there is the possibility that the supernovae will be microlensed. This situation was investigated by Schneider & Wagoner (1987) and Linder, Schneider & Wagoner (1988). Microlensing occurs when two images of the source are produced which are too close together to be individually resolved and can result in very high magnifications. If it occurs, the microlensing of supernovae is expected to be identifiable because the changing size of the supernova's photosphere makes the magnification time dependent and thus distorts the light-curve.

A supernova could also be lensed by one dominant galaxy cluster or individual galaxy. There is the possibility of getting multiple observable images and high magnifications (strong lensing) in this case. It has been suggested that observing supernovae behind galaxy clusters would be a way of lifting the mass sheet degeneracy that exists in shear measurements of the gravitational lensing (Kolatt & Bartelmann 1997). The likelihood of a supernova at $z = 1$ being strongly lensed by a galaxy or cluster is very small unless they are specifically sought out. In general a supernova will be lensed by many galaxies and larger structures that will each have a weak and roughly equal contribution to the total magnification. This will increase the dispersion of high redshift supernovae and decrease the precision of cosmological parameter determinations. This decrease in precision has been investigated by Frieman (1996) using analytic methods and by Wambsganss *et al.* (1997) using numerical models. In this paper the problem will be turned around and we will ask how well the lensing itself can be determined from the supernova data.

On the face of it using supernovae to look for gravitational lensing by LSS has a few disadvantages and few advantages over doing it with galaxies. For supernovae the signal to noise in each measurement can be much greater. Lensing is estimated to contribute about 5 to 10% to the observed root-mean-squared ellipticity of a $z = 1$ galaxy. For supernovae the variance in the lensing contribution is comparable to the intrinsic variance in the peak magnitude at this redshift. If this were the end of the story galaxy lensing would clearly win out due to superior numbers. But the unlensed ellipticity distribution of galaxies at high redshift is not known and can not be easily extrapolated from zero redshift galaxies. For this reason lensing must be inferred by correlations between galaxies, either between lensed galaxies or between lensed galaxies and foreground galaxies. The result is that galaxy lensing measures the shear averaged over a finite area on the sky. This average shear drops rapidly with increasing area and the signal to noise is reduced to something more like $10^{-6} - 10^{-5}$ per galaxy on the 0.1 deg^2 scale. This is made up for by the large number of evaluable galaxies ($\sim 10^5 \text{ deg}^{-2}$) to the extent that fluctuations in the projected mass density at $1 - 100 \text{ arcmin}$ scales are expected to be detectable in the near future. In contrast, the dispersion in the absolute magnitude of type Ia supernovae is presumably independent of redshift. The dispersion can then be measured in a low redshift population where lensing is not important. Galaxy lensing does have the advantage of sources that are generally at a higher redshift than is accessible to supernovae searches and strength of lensing increases with redshift. On the other hand, the redshift of distribution of faint galaxies is not strongly constrained which adds systematic uncertainty. The redshifts of supernovae are individually measured.

It is clear that supernova lensing and galaxy lensing probe different scales of density fluctuations. Since supernova lensing is a measure of the lensing at a point, not an average over a region on the sky, it will be sensitive to smaller scales. Supernova lensing is a direct measurement of the magnification which, in the

weak lensing limit, is related to the mass density in the line of sight only. The shear is dependent on the mass outside of the “beam” and is related to the projected mass density through a differential operator (Kaiser & Squires 1993) which makes it insensitive to any uniform offset - the “mass sheet degeneracy”. Galaxy lensing has the potential of measuring lensing over a range of scales. With the possible exception of supernovae viewed through galaxy clusters, it will be difficult to find enough supernovae that are close enough together to measure correlations between them.

In the next section I describe first how the lensing of supernovae is related to the density fluctuations and then I describe how the lensing signal could be identified in the data. In section 3 I use a model of structure formation to estimate the level of signal and to motivate some parameterizations. In the last section I make some concluding remarks about certain complications.

2. Formalism

In the next section I will show how the variance in the magnification of supernovae is related to the power spectrum of density fluctuations in the universe. In this section only a few loose and justifiable restrictions on the form of the density fluctuations will be required. In section 2.2, I consider an idealized model for lensing by an isolated galaxy. This model will be used for illustrative purposes in section 3. In section 2.3 a statistical method for handling the data and quantifying the lensing contributions is discussed. It is assumed throughout that the lensing is weak and multiple images are not produced. This assumption will be justified in section 3.

2.1. Background Magnification

Here I will calculate how the luminosities of supernovae are affected by background mass fluctuations. The lensing will be assumed to be weak throughout. It is to be expected that the variance of supernova magnitudes will be increased by lensing. In addition, if two or more supernovae are close enough together on the sky they will be lensing by coherent structures so there magnitudes will be correlated even if they are at different redshifts. Both of these effects will be calculated at once.

Lensing can be viewed mathematically as a mapping from points on a source plane to points on a image plane. The Jacobian matrix of this mapping can be written as the identity plus a perturbation, $J_{ij}(\theta) = \delta_{ij} + \Phi_{ij}(\theta)$. In the weak lensing limit the magnification is given by

$$\mu(\theta) = \det [\mathbf{I} + \Phi(\theta)]^{-1} \simeq 1 - \text{tr} \Phi(\theta) \quad (1)$$

It is standard practice to define the convergence, $2\kappa(\theta) \equiv -\text{tr} \Phi(\theta)$. The change in the magnitude of a point source is then

$$m - \overline{m} = 2.5 \log [\mu(\theta)] \simeq 2.1715\kappa(\theta). \quad (2)$$

To calculate correlations in $\kappa(\theta)$ I will use a perturbation method based on the techniques developed in (Gunn 1967), (Blandford *et al.* 1991), (Kaiser 1992). I will use the same notation as (Metcalf & Silk 1997). The angular deflection of an image can be written

$$\delta\theta_i(r) = -\frac{2}{g(r)} \int_0^r dr' g(r-r') \phi_{,i}(r'). \quad (3)$$

where r is the coordinate distance and $g(r) = \{R_c \sinh(r/R_c), r, R_c \sin(r/R_c)\}$ for the open, flat and closed global geometries respectively. The curvature scale is $R_c = |H_0 \sqrt{1 - \Omega - \Omega_\Lambda}|^{-1}$. Subscripts with commas in front of them denote partial derivatives and $\phi(x)$ is the potential in longitudinal gauge which is the same

as the dimensionless Newtonian potential in the present context. The shear tensor which measures the stretching of an infinitesimal image is given by

$$\Phi_{ij} \equiv \frac{\partial \delta \theta_i}{\partial \theta_j} = \frac{-2}{g(r)} \int_0^r dr' g(r') g(r-r') \phi_{,ij}(r'). \quad (4)$$

The coordinate distance is related to redshift by

$$r(z) = H_o^{-1} \int_0^z dz' [\Omega(1+z')^3 + (1-\Omega-\Omega_\Lambda)(1+z')^2 + \Omega_\Lambda]. \quad (5)$$

and the luminosity distance is $d_L(z) = (1+z)g(r(z))$ so that the average magnitude of a supernovae is $\overline{m}(z) = M_{Ia} + 5 \log d_L(z)$.

The convergence will on average be zero, but it will be different for each supernova. We need the correlation in the convergence of two sources at points θ_1 and θ_2 on the sky and at coordinate distances r_1 and r_2 .

$$\langle \kappa(\theta_1, r_1) \kappa(\theta_2, r_2) \rangle = \int_0^{r_1} dr' \frac{g(r') g(r_1 - r')}{g(r_1)} \int_0^{r_2} dr'' \frac{g(r'') g(r_2 - r'')}{g(r_2)} \langle \nabla_{\perp}^2 \phi(\theta_1, r') \nabla_{\perp}^2 \phi(\theta_2, r'') \rangle \quad (6)$$

It is useful to work in Fourier space at this point. If the potential is statistically homogeneous and isotropic the power spectrum of the potential is related to its Fourier coefficients by $P_\phi(k) = (2\pi)^3 \delta^3(\mathbf{k} - \mathbf{k}') \langle \tilde{\phi}_k \tilde{\phi}_{k'} \rangle$. The power spectrum of the potential is then related to the power spectrum of the mass density contrast by Poisson's equation, $P_\phi(k, \tau) = 9a(\tau)^{-2} \Omega_o^2 H_o^4 k^{-4} P(k, \tau)/4$ where $a(\tau)$ is the scale factor normalized to 1 at the present epoch.

The expression (6) can be significantly simplified by using an approximation that is equivalent to Limber's equation (Limber 1954). If the scales of the structures responsible for the lensing are much smaller than the distance to the source, any correlations in the radial direction will tend to wash out. This can be incorporated into the calculation by taking the correlation function of the potential to be a function of only \mathbf{x}_\perp or equivalently, the power spectrum of the potential to be a function of only k_\perp . This is a very good approximation for most realistic models of large scale structure. For a more detailed justification see the appendix of (Kaiser 1992) and (Metcalf & Silk 1997).

With Limber's approximation equation (6) can be reduced to

$$\begin{aligned} \langle \kappa(\theta_1, r_1) \kappa(\theta_2, r_2) \rangle &= \left(\frac{3}{2} \Omega_o H_o^2 \right)^2 \int_0^{r_1 < r_2} dr' \frac{g(r')^2 g(r_1 - r') g(r_2 - r')}{g(r_1) g(r_2)} \\ &\quad \times \int_0^\infty \frac{dk}{2\pi} a(\tau')^{-2} k P(k, \tau') J_o(g(r')|\theta_1 - \theta_2|k). \end{aligned} \quad (7)$$

where J_o is the zeroth order Bessel function. Note that no assumption of Gaussianity or linear evolution of structure has been used in deriving (7).

2.2. Lensing by Individual Galaxies

The mass density of an individual galaxy halo or a cluster of galaxies can to a very good approximation be considered to lie in a thin plane. From (4) it is easily found that $\kappa(\theta) = \Sigma(\theta)/\Sigma_c$ where $\Sigma(\theta)$ is the surface density of the object and the critical surface density is $\Sigma_c = (4\pi a_l g(r_l) g(r - r_l)/g(r))^{-1}$. The subscript l denotes quantities evaluated at the lensing object.

I will use the truncated isothermal sphere to describe galactic structure. Although this model is primitive and certainly not realistic in the central regions of the galaxy, it should be sufficient for my

purposes. A more advanced model could be straightforwardly incorporated if desired. The density of an isothermal sphere is $\rho(r) = \sigma_l^2/2\pi r^2$ where σ_l is the one dimensional velocity dispersion. The convergence is then

$$\kappa(R) = \frac{4\sigma_l^2}{R} \tan^{-1} \left(\frac{\sqrt{R_m^2 - R^2}}{R} \right) \left[a_l \frac{g(r_l)g(r - r_l)}{g(r)} \right], \quad R < R_m \quad (8)$$

and 0 for $R < R_m$. The radius of the sphere, R_m , can be related to the total mass by $M = 2\sigma_l^2 R_m$.

The probability of the convergence being bigger than κ for a particular supernovae is

$$P(> \kappa) = \pi \int_0^\infty d\sigma_l \int_0^r dr' \frac{dn}{d\sigma_l}(\sigma_l, r') \frac{R(r', R_m, \sigma_l, \kappa)^2}{a(r')^2} \quad (9)$$

where $R(r', R_m, \sigma_l, \kappa)$ is the solution to (8) and $n(\sigma_l, r)$ is the comoving number density of lenses with velocity dispersion σ_l . In calculations, $R(r', R_m, \sigma_l, \kappa)$ will be found numerically. I will use this result in section 3 to gain some insight into origin of skewness in the magnification distribution. Strictly speaking (9) is actually an overestimate of the probability that the convergence is greater than κ . This is because it is a probability over lines of sight. The appropriate probability is over sources which are less likely to be in areas of higher magnification. However if the magnification is small the difference between the two probabilities is not significant.

In contrast to the convergence the shear will not be zero outside the sphere. The shear is defined as $\gamma^2 = \frac{1}{4}(\Phi_{11} - \Phi_{22})^2 + \Phi_{12}^2$. Outside the isothermal sphere, $R > R_m$, $\gamma = \frac{M}{2\pi^2 \Sigma_c R^2}$. In the same region the magnification is $\mu = (1 - \gamma^2)^{-1} \simeq 1 + \gamma^2$ which in accordance with the weak lensing limit and with realistic galaxy models is negligible. This demonstrates how shear measures of weak lensing are not direct measures of the local mass density and how they will be less sensitive to the rapid changes in the density.

If the impact parameter is small enough the supernova will be strongly lensed and expression (9) will not be valid. These cases can be modeled individually, but they should not be used for cosmological parameter determination. As will be shown these cases should be rare and easily identified by the proximity of a foreground galaxy or cluster to the supernova. For this paper I will assume that these rare cases of strong lensing are removed from or do not occur in the sample of observed supernovae.

2.3. Measuring Parameters

The question I will address here is how to measure the parameters of a model using the supernova data. And conversely, we want to know the amount and quality of the data that will be necessary to measure parameters to a given accuracy. To do these things I use a likelihood analysis approach which begins with defining a likelihood function. The distribution of κ is not expected to be Gaussian. Nonlinear clustering causes the distribution to be skewed in favor of demagnification. This is simply because the mass is concentrated into small regions so a typical line of sight will tend to travel disproportionately through underdense regions. The distribution of corrected, intrinsic magnitudes may not be Gaussian either although at present the low redshift supernovae are consistent with Gaussian after correcting for extinction. Extinction corrections are more difficult for high redshift supernovae so non-Gaussianity may be introduced in this way. However one expects that the distribution of Δm will be close to Gaussian because it is the result of several independent random processes. To account for the small deviation from Gaussianity the second term of the Edgeworth expansion of the probability function is included (see for example Cramér (1946) and Juszkiewicz *et al.* (1995)). This gives the distribution a possibly measurable skewness.

The perturbed Gaussian likelihood function is

$$\mathcal{L} = \frac{1}{\sqrt{(2\pi)^n \det \mathbf{C}}} \exp\left(-\frac{1}{2} \mathbf{\Delta m}^T \mathbf{C}^{-1} \mathbf{\Delta m}\right) \prod_i \left[1 + \frac{1}{6} \mu_i^3 H_3\left(\frac{\Delta m_i}{\sigma_i}\right)\right], \quad \sigma_i^2 = 4.715\langle\kappa_i^2\rangle + (\sigma_m^2)_i \quad (10)$$

where $\Delta m_i \equiv m_i - \bar{m}_i$, the difference between the observed and expected magnitudes, and \mathbf{C} is the covariance matrix as predicted by the model. The subscripts correspond to each of the supernovae observed. I will divide the covariance matrix into two parts, the first due to lensing and the second due to other sources of dispersion in supernova peak luminosities - $C_{ij} = 4.715\langle\kappa_i\kappa_j\rangle(z) + (\sigma_m^2)_i\delta_{ij}$. The diagonal elements are the σ_i 's. In turn we can divide $(\sigma_m^2)_i = \sigma_M^2 + (\sigma_n^2)_i$ where σ_M is the variance in the intrinsic peak magnitude which is the same for all supernovae and $(\sigma_n^2)_i$ is the variance due to noise, light-curve fitting, etc. There is no sum over repeated indices. Maximizing (10), or its log, with respect to all the model parameters will result in the set of parameters that best fit the data. Constraints from other, independent determinations of parameters could be incorporated into the likelihood function with a prior distribution.

In (10) $H_3(x)$ is the third Hermite polynomial normalized so that

$$\int_{-\infty}^{\infty} dx H_l(x) H_m(x) e^{-x^2/2} = \begin{cases} 0 & l \neq m \\ \sqrt{2\pi} l! & l = m \end{cases} \quad (11)$$

The parameter μ_i^3 is the skewness of the Δm_i distribution. It is related to the third moment, M_i^3 , by $\mu_i^3 = M_i^3/\sigma_i^3$. The third moments of the distributions add so if both the lensing and the intrinsic Δm distributions have a third moment

$$\mu_i^3 \sigma_i^3 = 4.715\langle\kappa_i^2\rangle^{3/2} \mu_{\kappa i}^3 + \sigma_m^3 \mu_m^3. \quad (12)$$

Just like in the case of the variance, the skew due to lensing could be differentiated from the intrinsic skew by its redshift dependence. I will ignore any skew that might be in the correlation between supernovae. This is likely to be very small and it is not likely that it could be meaningfully constrained by observations. The existence of skewness in the true distribution of κ will not change the maximum of the likelihood function by very much (order μ^6) so the set of most likely parameters as derived with the purely Gaussian likelihood function will not differ greatly from those derived with skewness included unless the skewness itself is a function of those parameters.

If the correlations between the lensing of different supernovae are ignored the covariance matrix is diagonal. In section 3 I will show that this is probably a good approximation. The likelihood function simplifies in this case to

$$\ln \mathcal{L} = \frac{1}{2} \sum_i \left[(\Delta m_i)^2 (4.715\langle\kappa_i^2\rangle + (\sigma_m^2)_i)^{-1} + \ln (4.715\langle\kappa_i^2\rangle + (\sigma_m^2)_i) + \ln (1 + \mu_i^3 H_3(\Delta m_i/\sigma_i)) \right]. \quad (13)$$

Now I turn to the problem of estimating the precision with which cosmological or model parameters will be determined. The precision can be estimated by the ensemble average of the Fisher matrix which is made of the second derivatives of the likelihood function with respect to those parameters. To simplify things I will assume that the skewness, μ_i^3 , is not a function of the parameters of interest. Then if we consider two parameters α and β ,

$$\left\langle -\frac{\partial^2 \ln \mathcal{L}}{\partial \alpha \partial \beta} \right\rangle = \langle (\alpha - \bar{\alpha})(\beta - \bar{\beta}) \rangle_{\mathcal{L}}^{-1} = \text{tr} \left[\bar{\mathbf{m}}_{,\alpha} \bar{\mathbf{m}}_{,\beta}^T \mathbf{C}^{-1} + \frac{1}{2} \mathbf{C}^{-1} \mathbf{C}_{,\alpha} \mathbf{C}^{-1} \mathbf{C}_{,\beta} + \frac{1}{6} \mu_{,\alpha\beta}^3 \right]. \quad (14)$$

The first term in this expression is the usual term that comes from uncertainties in measuring the mean magnitude of the supernovae and the second term is the result of the dispersion of the magnitudes, due to

lensing or other things, being a function of the parameters being measured. If the supernovae are taken to be statistically independent (14) simplifies to

$$\langle(\alpha - \bar{\alpha})(\beta - \bar{\beta})\rangle_{\mathcal{L}}^{-1} = \sum_i (4.715\langle\kappa_i^2\rangle + (\sigma_m^2)_i)^{-2} \left\{ \overline{m}_{i,\alpha} \overline{m}_{i,\beta} (4.715\langle\kappa_i^2\rangle + (\sigma_m^2)_i) + \frac{(4.715)^2}{2} \langle\kappa_i^2\rangle_{,\alpha} \langle\kappa_i^2\rangle_{,\beta} \right\}. \quad (15)$$

We can also find the estimated uncertainty in the skewness. To first order in μ_i^3 , $\langle(\mu_i^3 - \langle\mu_i^3\rangle)^2\rangle^{-1} = N_i$.

3. Scalings, Models and Predictions

To make some quantitative and qualitative estimates I use models whose mass density is dominated by cold dark matter (CDM). It is helpful to first consider what might be expected for the form of the lensing signal. In linear theory $P_L(k, a(\tau)) \propto [a(\tau)g(\Omega(\tau), \Omega_\Lambda(\tau))]^2$ where $g(\Omega, \Omega_\Lambda)$ is given in (Carroll, Press & Turner 1992). This allows the integral in (7) to decouple so that factors dependent on the power spectrum can be separated from factors dependent on cosmological parameters. The same thing happens in the opposite extreme when structure is highly nonlinear and fully virialized. In this case structure is stable in real space and the power spectrum evolves like $P_{NL}(k, a(\tau)) \propto a(\tau)^3$ regardless of cosmological parameters. These two extreme cases can be explicitly calculated for the $\Omega = 1$ model where $P_L(k, a(\tau)) \propto a(\tau)^2$,

$$\langle\kappa(z)^2\rangle = \frac{3}{40} (r(z)H_o)^3 H_o \int_0^\infty \frac{dk}{2\pi} k P(k) \times \begin{cases} 1 & \text{linear evolution} \\ 1 - \frac{1}{2}r(z)H_o + \frac{1}{14}[r(z)H_o]^2 & \text{stable evolution} \end{cases} \quad (16)$$

where the power spectrum is evaluated at the present day. These two results bracket the real result for $\Omega = 1$ models - linear evolution bounds it at the top and stable evolution on the bottom. The same thing can be done for $\Omega \neq 1$ models. In this way if $\langle\kappa^2\rangle$ is measured firm bounds on the integral of $kP(k)$ can be found within a model. The model will already be strongly constrained by $\overline{m}(z)$ and other observations. If the redshift dependence of $\langle\kappa^2\rangle$ could be firmly established insight into the evolution of clustering would be gained. For $\Omega \neq 1$ models $P_L(k, a(\tau))$ is a somewhat steeper function of $r(z)$ because of the decay of potential fluctuations. The stable clustering case is less strongly dependent on Ω except for the Ω^2 factor in (7) which comes from Poisson's equation. The geometric factors in $\Omega + \Omega_\Lambda \neq 1$ models will tend to make $\langle\kappa(r)^2\rangle$ steeper, all other things being equal.

To make things more quantitative I use the linear power spectrum of matter fluctuations given by (Sugiyama 1995):

$$P(k) = Ak^n T(ke^{\Omega_b + \Omega_b/\Omega}/\Omega h^2)^2 \quad (17)$$

$$T(q) = \frac{\ln(1+2.34q)}{2.34q} [1 + 3.89q + (16.1q)^2 + (5.46q)^3 + (6.71q)^4]^{-1/4}$$

To convert this to a nonlinear power spectrum I use the technique of (Peacock & Dodds 1996) which is based on N-body simulations and thus does not take into account any hydrodynamics that might be important on small scales. In all calculations $\Omega_b = 0.015h^{-2}$. This power spectrum goes to k^{-3} at small scales so that the dimensionless power spectrum $k^3 P(k)$ becomes scale independent. Figure 1 shows what range in k -space is responsible for lensing in these models. The power spectrum in this range is speculative. I consider this only a toy model to be used to estimate the magnitude of signals and noise and as an example of how to parameterize the effects. The goal is of course to measure the lensing effects in a relatively model independent way. I choose to cut the power spectrum off at $k = 1000 \text{ Mpc}^{-1}$ for the purposes of (7). A cutoff at $k = 100 \text{ Mpc}^{-1}$ reduces $\langle\kappa^2\rangle$ by $\sim 10 - 18\%$.

I have found a convenient fit to the variance of the convergence in these models

$$\langle\kappa(z)^2\rangle \simeq \eta_o^2 [r(z, \Omega, \Omega_\Lambda)H_o]^\gamma \quad (18)$$

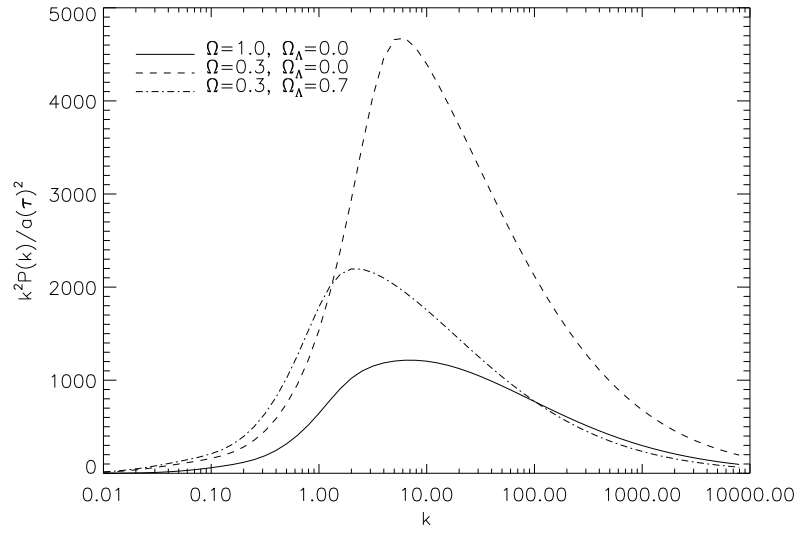


Fig. 1.— The scale dependence of the lensing of point sources in CDM models.

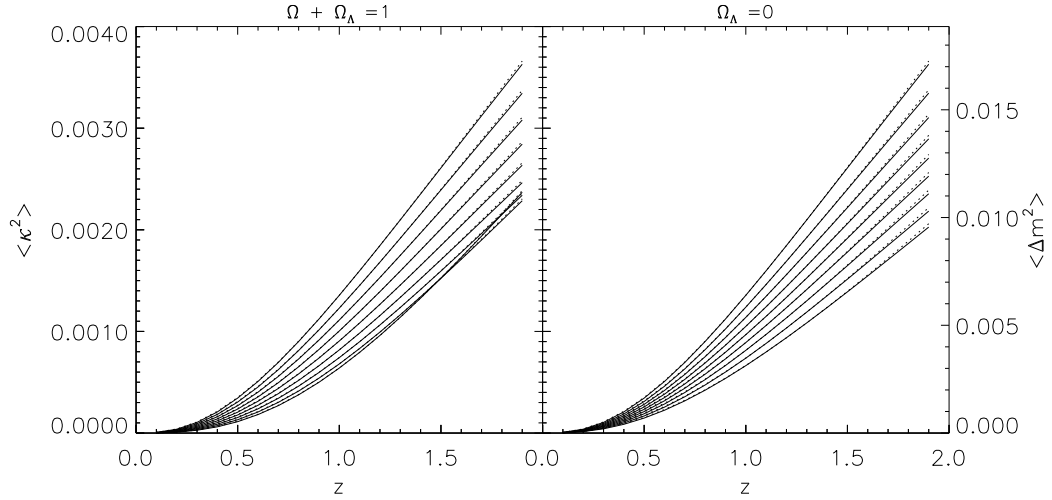


Fig. 2.— The second moment of κ in CDM models. On the left are flat models and on the right, open models. The dotted curves are the fits given in the text. The top curve in each plot is for $\Omega = 1$. Each successive curves going down has Ω reduced by 0.1 from the one above it. All the models have the normalization that best fits galaxy cluster abundances and $h = 0.6$.

where $r(z, \Omega, \Omega_\Lambda)$ is the coordinate distance. This fits all the $k < 1000 \text{ Mpc}^{-1}$, cluster-normalized CDM models reasonably well with $\gamma \simeq 2.92$ for flat models and $\gamma \simeq 2.80 + 0.11\Omega$ for $\Omega_\Lambda = 0$ models as is shown in figure 2. The constant η_o depends on how the power spectrum is normalized. If it is normalized to cluster abundances using the formulae of (Viana & Liddle 1996) with $h = 0.6$ I get $\eta_o^2 \simeq (0.70 + 1.44\Omega^2)h \times 10^{-2}$ for $\Omega_\Lambda = 0$ models and $\eta_o^2 \simeq (0.32 + 1.80\Omega^2)h \times 10^{-2}$ for flat models. The convergence does not have a simple dependence on H_o because both the power spectrum's normalization and shape are dependent on it. If the normalization is kept constant and Ω is varied independently, η_o is a steeper function of Ω , but this normalization will always be inconsistent with other observations for some range of Ω . To properly incorporate independent constraints on the normalization (or any other parameter), a prior distribution should be incorporated in the likelihood function, (10). As is expected from the discussion above, $\langle \kappa(z)^2 \rangle$ falls somewhere between stable and linear evolution for all the models.

Figure 3 shows the angular dependence of $\langle \kappa(\theta_1)\kappa(\theta_2) \rangle$. The correlations between supernovae will be very small if they are separated by more than about an arc-minute. It is unlikely that enough supernovae can be found close enough together for this cross-correlation to be measured. The large angular sizes and high densities of galaxy clusters make them an exception to this role, but a random line of sight is not likely to pass through a cluster. If these cross-correlations could be measured it would be sensitive to density structures of a larger scale than the diagonal elements, $\langle \kappa_i^2 \rangle$.

To estimate how well η_o can be measured we can use (15) to find

$$\langle (\eta_o - \langle \eta_o \rangle)^2 \rangle_{\mathcal{L}}^{-1} = \frac{1}{2} \sum_i \left[\frac{9.43\eta_o(r_i H_o)^\gamma}{4.715\eta_o(r_i H_o)^\gamma + \sigma_m^2} \right]^2. \quad (19)$$

Table 1 gives estimates of the numbers of supernovae needed to make a 2σ detection of $\langle \kappa^2 \rangle$ calculated using (15). The supernovae are taken to all be at the same redshift, $z = 0.5$, $z = 1.0$ and $z = 1.5$. The numbers $N_{0.10}$ are for $\sigma_m = 0.1$. The number goes as σ_m^4 so it is very sensitive to this parameter.

Of course the supernovae will not all be at the same redshift and the “intrinsic” variance, σ_m , in the supernova magnitudes will not be perfectly determined. It makes sense to try to determine both σ_m and η_o at the same time. One way to visualize how well this could be done is to plot $\langle \ln \mathcal{L}(\eta_o, \sigma_m) \rangle$. The curves at 0.5 and 2 less than the maximum are estimations of the boundaries of the 68% and 95% confidence regions. This is plotted in figure 4. The redshift distribution of the supernovae is taken to be proportional to comoving volume with a cutoff at $z = 1.3$. This is an idealization which assumes that the observed supernova rate and the detection efficiency are not functions of redshift, but the magnitude limit is conservative. A separate population of 25 $z \simeq 0$ supernovae is also included because searches for low redshift supernovae are done by targeted observations as opposed to searches for high redshift supernovae which can be done either by cataloging galaxies or by differencing multiple observations of more or less random fields. Figure 5 illustrates how going to higher redshift can help in differentiating between models. The σ_8 normalizations given in figure 4 and 5 are for the linear power spectra. Changes in the linear normalization are magnified in the nonlinear power spectrum so that they show up strongly in the lensing. This can be seen in the $\sigma_8 = 0.8$, $\Omega = 1$ model which is still consistent with cluster abundances. Low Ω models have significantly lower η_o 's than high Ω with the same linear normalization or with cluster normalization which increases with lower Ω . This is largely because of the factor of Ω^2 in $\langle \kappa^2 \rangle$. Models with the same Ω but different Ω_Λ are not strongly discriminated between. Getting to high redshift will be important for discriminating between models because the higher the redshift the less elongated the likelihood contours are along the η_o axis.

The rate at which high redshift supernovae can be discovered is limited by the rate at which they occur, the area on the sky that is surveyed and the efficiency with which they can be detected. Although the rate of star formation at high redshift can be estimated from observations (Madau *et al.* 1996), the type Ia supernovae are expected to lag significantly behind it. The amount of time required for a white dwarf to

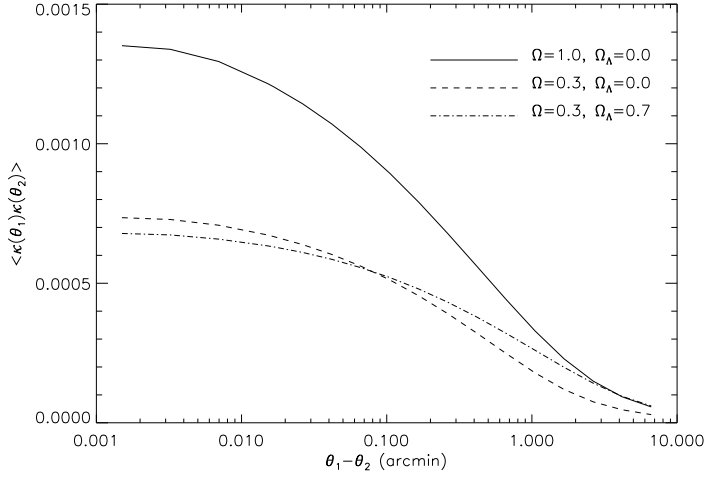


Fig. 3.— The second moment of the convergence as a function of angular separation between sources. All cases are for cluster normalized CDM models with $h = 0.6$ and the sources are at $z = 1$.

Table 1. Number of Supernovae Needed for Detection

Model				$z = 0.5$			$z = 1.0$			$z = 1.5$		
Ω	Ω_Λ	σ_8	h	$\langle \kappa^2 \rangle$	Δm	$N_{0.1}$	$\langle \kappa^2 \rangle$	Δm	$N_{0.1}$	$\langle \kappa^2 \rangle$	Δm	$N_{0.1}$
1.0	0.0	0.6	0.60	3.4×10^{-4}	0.04	103	1.4×10^{-3}	0.08	13	2.6×10^{-3}	0.11	7
1.0	0.0	0.6	0.75	4.6×10^{-4}	0.05	62	1.8×10^{-3}	0.09	9	3.5×10^{-3}	0.13	5
1.0	0.0	0.5	0.65	2.1×10^{-4}	0.03	252	8.1×10^{-4}	0.06	26	1.6×10^{-3}	0.09	11
1.0	0.0	0.8	0.65	7.0×10^{-4}	0.06	33	2.8×10^{-3}	0.11	6	5.4×10^{-3}	0.16	4
0.3	0.0	1.0	0.60	1.7×10^{-4}	0.03	370	7.4×10^{-4}	0.06	30	1.5×10^{-3}	0.08	11
0.3	0.0	1.0	0.75	2.0×10^{-4}	0.03	261	9.0×10^{-4}	0.06	23	1.8×10^{-3}	0.09	9
0.3	0.0	0.7	0.65	8.2×10^{-5}	0.02	1456	3.5×10^{-4}	0.04	97	7.3×10^{-4}	0.06	31
0.3	0.0	1.4	0.65	3.7×10^{-4}	0.04	89	1.7×10^{-3}	0.09	10	3.4×10^{-3}	0.13	5
0.3	0.7	1.2	0.60	1.3×10^{-4}	0.02	592	6.8×10^{-4}	0.06	34	1.5×10^{-3}	0.08	11
0.3	0.7	1.2	0.75	1.5×10^{-4}	0.03	432	8.1×10^{-4}	0.06	26	1.8×10^{-3}	0.09	9
0.3	0.7	0.8	0.65	6.3×10^{-5}	0.02	2419	3.2×10^{-4}	0.04	114	7.2×10^{-4}	0.06	31
0.3	0.7	1.6	0.65	2.9×10^{-4}	0.04	139	1.5×10^{-3}	0.08	11	3.4×10^{-3}	0.13	5

Note. — These are 2σ detection limits.

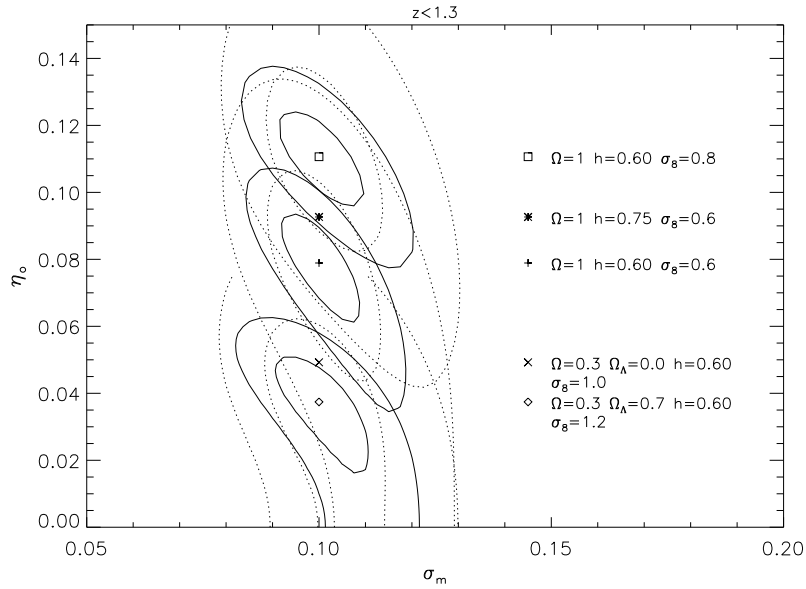


Fig. 4.— The estimated confidence regions for the combination of lensing and “intrinsic” variance in the supernovae magnitudes. Solid curves are for 68% and 95% confidence regions with 25 zero redshift and 250 high redshift supernovae. The dotted lines are the same for 25 zero redshift and 50 high redshift supernovae. The high redshift supernovae are distributed according to comoving volume with none having a redshift exceeding $z = 1.3$.

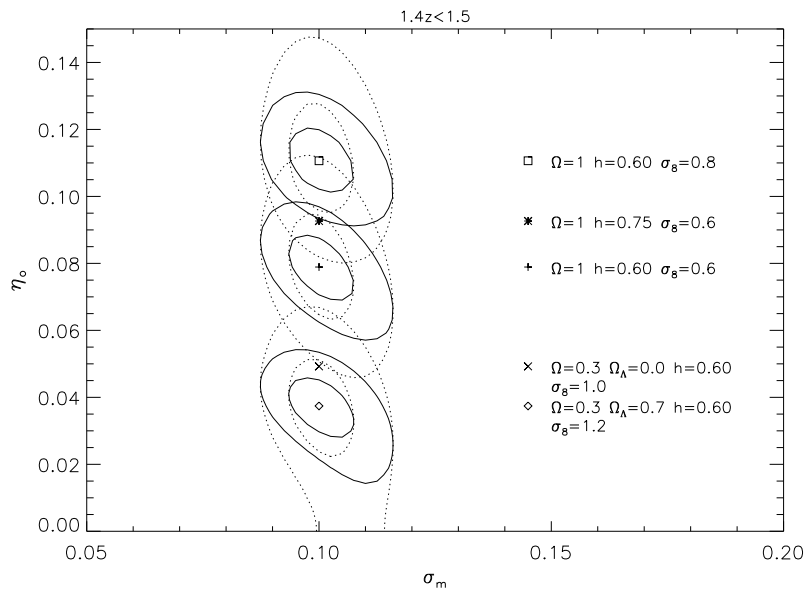


Fig. 5.— Same as in figure 4, but with 50 (dotted) and 150 (solid) supernovae between $z=1.4$ and $z=1.5$. In both cases there are 100 zero redshift supernovae.

accrete enough material to go supernova is not only unknown, but probably varies greatly on a case to case basis. There is one measurement of the Ia supernova rate at $z \sim 0.4$ which is $34.4_{-16.2}^{+23.9} \text{ yr}^{-1} \text{deg}^{-2}$ (Pain *et al.* 1996). If the rest frame rate per comoving volume remains constant the observed rate of supernovae at z is $R(z) = R_o(1+z_o)g(r(z))^2/(1+z)g(r(z_o))^2$ which makes it 2 or 3 times larger at $z = 1$. More thoughtful estimations predict that the rest frame rate per comoving volume will go up by a factor of 1 to 2.5 (Sabat *et al.* 1997, Ruiz-Lapuente & Canal 1998). This makes detecting hundreds of high redshift supernovae possible within a few years. (The Supernova Cosmology Project (Perlmutter *et al.* 1997) currently surveys $\sim 3 \text{ deg}^2$.)

Some insight can be gained by using (9) to calculate the probability that a supernova will be magnified by more than the $2.171\langle\kappa^2\rangle^{1/2}$ calculated above by a single galaxy. If all the galaxies are taken to be the same mass and have the same velocity dispersion and their comoving number density does not change I find $P(> 0.05) = (0.1 - 0.6)\Omega_g$ for $M = 10^{12} \text{ M}_\odot$ and $\sigma_l = 150 \text{ km s}^{-1}$ where Ω_g is the density of matter in galaxies relative to critical density. For 2σ events the probability drops to $(0.07 - 0.2)\Omega_g$. For $M = 10^{11} \text{ M}_\odot$, I get $(0.07 - 0.1)\Omega_g$ and $(0.03 - 0.06)\Omega_g$. The mass density in the luminous part of large luminous galaxies can be estimated from observations, $\Omega_g \lesssim 0.005$. The total mass in galaxies might be an order of magnitude larger. This means that in this model certainly less than one percent of the supernovae will be close enough to a galaxy to have it magnified to the level of the variance. Close encounters with galaxies are rare. Decreasing the velocity dispersion of the halos makes them larger and more diffuse. This decreases the probability that there will be a high magnification event because $R(r', R_m, \sigma_l, \kappa)$ in (9) decreases. Because there are no compensating objects of high negative mass density most supernovae will be weakly demagnified. Fewer will be weakly magnified and there will be a small number with magnifications of several times the variance. This is the origin of the skewness in the lensing distribution. If the structures are diffuse, low σ_l , the skewness, μ^3 , will be negative and small in absolute value. If the structures are compact, $-\mu^3$ will be large. Truly strong lensing, $\kappa \gtrsim 1$, will be even more rare.

These calculations of $\langle\Delta m^2\rangle$ agree well with those of Frieman (1996). The numerical simulations of (Wambsganss *et al.* (1997), Wambsganss *et al.* (1998)) give somewhat smaller values. This is probably due to the combination of their using the COBE normalization which is smaller than the cluster normalization for low Ω models and their simulation having a resolution of $\sim 13h^{-1} \text{ kpc}$ ($k \sim 480h \text{ Mpc}^{-1}$). The distribution they find for the magnification does have a negative skewness, but they do not give numerical values.

4. Conclusions

It has been shown that measuring the gravitational lensing of type Ia supernovae is feasible if the noise can be reasonably constrained. It would be best to solve for the best fit cosmological parameters (ie. Ω , Ω_Λ), lensing strength (ie. η_o^γ) and intrinsic noise (σ_M) simultaneously using supernovae at all redshifts. The photometric uncertainties should be comparatively well determined for each supernova. One could then marginalize over the intrinsic variance, σ_M . The greatest worry is that the type Ia supernovae properties or their galactic environments are changing with time. Observations of spectral features and colors (Perlmutter *et al.* 1997) along with theoretical models for the explosion mechanism suggest that this should not be the case, but the possibility remains. Perhaps the greatest worry for cosmological parameter estimation is extinction which will systematically reduce $\bar{m}(z)$, increase its dispersion and make its distribution non-Gaussian. Extinction should be accompanied by reddening which could be detected by observing in multiple colors, but the extinction law is not certain. There is no particularly compelling reason to believe that the dispersion introduced by extinction should systematically increase with redshift (although the correction becomes less certain) and thus the detection of lensing may not be strongly affected. But this important systematic certainly needs to be better understood. The methods discussed here could be used

to look for any redshift dependent change in the dispersion. With a model for how lensing changes as a function of redshift it is hoped that any other evolution could be distinguish from it.

There are some technical difficulties that put limits on the range of redshifts that are presently accessible for a supernova search. The region of the spectrum that is used to do the light curve correction passes out of the visible at $z \gtrsim 1$. To go to significantly higher redshift may require switching to the IR. There is also some uncertainty in the K-correction. But with all this in mind it seems that gravitational lensing of supernovae could be detectable in the next few years when hundreds of high redshift supernovae are observed and systematic effects are better understood. Pushing to higher redshift will be necessary and reducing the corrected, intrinsic magnitude dispersion, σ_m , would be highly beneficial. CCD cameras with fields of view approaching a square degree and very small pixel sizes are being built now. They will be used for weak lensing measurements using galaxy shear. Supernovae searches could be incorporated into these surveys with the benefit of improved cosmological parameter estimation and complimentary weak lensing measurements.

Combined with the limits on the cosmological parameters the lensing of supernovae can strongly constrain the power spectrum of the true mass density, unbiased by the light distribution, on the scale of galaxy halos. At present the mass distribution on these scales is not well known with the exception of within galaxy clusters which are certainly atypical regions. In addition the variance of the magnification distribution the skewness would provide an important constraint on the nature of structure in the nonlinear regime. It is not easy to make accurate predictions of how large this signal will be and this is not addressed in this paper. Very high resolution numerical simulations could be used to do this. However the skewness would probably contain information on structure at the scale of galaxy halos which are not easily resolved in simulations of structure formation.

Finally it should be mentioned that there are a few other ways in which one might hope to measure the gravitational lensing of supernovae. Unfortunately most of these are stymied by the small number of Ia supernovae that can be detected in reasonable amount of time. The correlations in the magnitude of different supernovae are unlikely to be strong enough to be statistically significant in the near future because of the lack of close pairs. The cross-correlation of supernova magnitudes and foreground galaxies counts which would be dependent on lensing and the bias is dominated by the Poisson noise introduced by the discreet nature of the galaxies.

I would like to thank J. Silk, A. Jaffe, S. Perlmutter and R. Pain for very useful discussions. This work was financially supported by NASA.

REFERENCES

Blandford,R.D, *et al.*, 1991, MNRAS, 251, 600.

Branch D., Nugent P. & Fisher A., 1997, *Thermonuclear Supernovae*, ed. P. Ruiz-Lapuente, R. Canal & J. Isern (Dordrecht:Kluwer), 715.

Carroll S.M., Press W.H. & Turner E.L., 1992, ARA&A, 30, 499.

Cramér H., 1946, *Mathimatical Methods of Statistics* (Princeton:Princeton Univ. Press).

Frieman J.A., 1996, Comments on Astrophysics??,astro-ph/9608068.

Gunn, J.E., 1967, ApJ, 150, 737.

Garnavich, P.M., 1998, ApJ, 493, L53.

Hammuy M., Phillips M.M., Suntzeff N.B., Schommer R., Maza J. & Aviles R., 1996, ApJ, 112, 2391.

Juszkiewicz R. *et al.*, 1995, ApJ, 442, 39.

Kaiser, N., 1992, ApJ, 388, 272.

Kaiser, N., 1996, submitted to ApJ, astro-ph/9610120.

Kaiser, N. & Squires G., 1993, ApJ, 404, 441.

Kolatt T.S. & Bartelmann M., 1997, astro-ph/9708120.

Limber, D.N., 1954, ApJ, 119, 665.

Linder E.V., Schneider P. & Wagoner R.V., 1988, ApJ, 324, 786.

Madau P. *et al.* 1996, MNRAS, 283, 1388.

Metcalf, R B & Silk, J, 1997, ApJ, 489, 1.

Mould, J. *et al.*, 1994, MNRAS, 271, 31.

Nugent P., Phillips M., Baron E., Branch E. & Hauschildt P., 1995, ApJ, 455, L147.

Pain R. *et al.*, 1996, ApJ, 473, 356.

Peacock J.A. & Dodds S.J., 1996, MNRAS, 280, L19.

Perlmutter S., *et al.*, 1997, ApJ, 483, 565.

Perlmutter S., *et al.*, 1998, Nature, 391, 51.

Pozzetti L., Bruzual A.G. & Zamorani G., 1996, MNRAS, 281, 953.

Ruiz-Lapuente P. & Canal R., 1998, astro-ph/9801141.

Riess A.G., Press W.H. & Kirshner R.P., 1996, ApJ, 473, 88.

Sabat R., Blanchard A., Guiderdoni B. & Silk J., 1997, astro-ph/9712065.

Schneider P. & Wagoner R.V., 1987, ApJ, 314, 154.

Sugiyama N., 1995, ApJS, 100, 281.

Valdes F., Tyson J. & Jarvis J., 1983, ApJ, 271, 431.

Viana, P.T.P. & Liddle, A.R., 1996, MNRAS, 281, 323.

Villumsen J.V., 1996, MNRAS, 281, 369.

Wambsganss J., Cen R., Xu G., & Ostriker J.P., 1997, ApJ, 475, L81.

Wambsganss J., Cen R., & Ostriker J.P., 1998, ApJ, 494, 29.